Eur. Phys. J. B **5**, 203–214 (1998)

THE EUROPEAN PHYSICAL JOURNAL B

© EDP Sciences
Springer-Verlag 1998

Interfacial polarisation effect on the interlayer couplings in Co/Rh sandwiches

A. Dinia[1,a], S. Zoll[1], M. Gester[1,b], D. Stoeffler[1], J.P. Jay[1], K. Ounadjela[1], H.A.M. van den Berg[2], and H. Rakoto[3]

[1] IPCMS-GEMME[c], 23 rue du Loess, 67037 Strasbourg, France
[2] Siemens AG, ZFE T MR 1, P.O. Box 3220, 91050 Erlangen, Germany
[3] SNCMP[d], INSA, Complexe Scientifique de Rangueil, 31077 Toulouse, France

Received: 18 February 1998 / Received in final form: 30 April 1998 / Accepted: 29 May 1998

Abstract. The structural, magnetic and transport properties of Co/Rh sandwiches grown by ultra high vacuum evaporation and sputtering have been studied. High-energy electron diffraction observations during the growth reveal that both Co and Rh layers have been stabilised in the (111) fcc structure for the evaporated sandwiches. X-ray measurements performed on sputtered samples show a predominant fcc polycrystalline structure of the stacks with a preferential (111) texture. Magnetisation and magnetoresistance measurements show a very strong antiferromagnetic exchange coupling for thin Rh layers, reaching 39 erg/cm^2 for 4.8 Å Rh, the strongest ever observed in exchange coupled systems. This value is in good agreement with the value of 38 erg/cm^2 obtained by *ab initio* calculations for Co/Rh (hcp) superlattices. This is explained by the magnetic nature of the Co/Rh interfaces. Indeed, the variation of the measured saturation magnetisation as a function of the Co layer thickness shows no evidence of Co moment reduction for the Co atoms located at the interfaces, even for the very thin layers. The value of the preserved magnetic moments of the cobalt atoms at the interfaces is confirmed by *ab initio* calculations for Co/Rh superlattices taking the intermixing into account.

PACS. 75.70-i Magnetic films and multilayers – 75.70.Cn Interfacial magnetic properties (multilayers, magnetic quantum wells, superlattices, magnetic heterostructures) – 75.70.Pa Giant magnetoresistance

1 Introduction

The discovery of the interlayer exchange coupling in magnetic multilayers [1] has stimulated a great number of fundamental studies as well as application-oriented research in the field of recording heads and magnetic sensors. Parkin *et al.* [2] first reported a large antiferromagnetic coupling of the order of 5 erg/cm^2 for magnetic Co films separated by a non magnetic Ru spacer. Other groups then studied the Co/Ru system using different preparation techniques and have shown the effect of preparation conditions on the antiferromagnetic coupling strength [3, 4]. It has been found that MBE grown Co/Ru multilayers show a stronger exchange coupling [4] than samples prepared by sputtering or by any other method. Such observations are in good agreement with theoretical works which showed that the strength of the coupling depends on the geometry of the Fermi surface [5], and as a consequence is very sensitive to the structural quality of the samples. Morover, Mathon *et al.* [6], by using detailed tight-binding calculations of the coupling, have shown that a mismatch between the ferromagnetic and spacer layer *d* bands, which increases with increasing number of holes in the band of the spacer, leads to a systematic variation of the coupling strength across the transition metal series in agreement with Parkin's results [7].

The aim of this work is to confirm that the interlayer coupling strength effectively increases by increasing the number of conduction electrons in the d band and that it depends considerably on the magnetic nature of the magnetic/non-magnetic interfaces. For the first time, we show the correlation between the exchange coupling strength and the nature of the magnetic/nonmagnetic interfaces. The large difference in coupling strengths between Co/Rh and Co/Ru for very thin spacer layers,

[a] e-mail: aziz@atlas.u-strasbg.fr
[b] *Present address:* Department of Physics, University of York, York Y01 5DD, U.K.
[c] UMR 46 CNRS-ULP.
[d] UMS 819 CNRS-UPS.

"7-8 times larger in the Co/Rh system" makes these two systems particularly appropriate for this topic. Such a large difference between these two systems cannot be solely attributed to the additional electron in the Rh "*d*" band but can only be explained by taking into account the nature of the magnetic/nonmagnetic interfaces. In fact, a strong reduction in the magnetism of the interfaces is observed and accounted for in terms of a 2 Å thick magnetically dead Co at each interface for Co/Ru, while the magnetization is preserved at the Co/Rh interfaces. This result is further confirmed by first principles electronic structure calculations.

This paper is organised as follows. Section 2 is devoted to the preparation conditions and structural characterisation through Reflection High Energy Electron Diffraction (RHEED), X-ray diffraction (XRD) and Nuclear Magnetic Resonance (NMR). The structural analysis is relevant to the understanding of the interlayer coupling strength which is strongly dependent on the structure of the layers and on the nature of the magnetic/non-magnetic interfaces. The study of the magnetic and transport properties will be presented in Section 3. After a brief description of the experimental techniques used, we present the variation of the interlayer coupling strength for both series of sandwiches as a function of the Rh spacer layer thickness. Then we focus our discussion on the giant interlayer coupling strength observed for MBE grown Co/Rh sandwiches that reaches 39 erg/cm^2 for a Rh thickness of about 5 Å. To clearly understand the origin of this giant coupling energy which is approximately ten times larger than the highest value observed in sputtered Co/Rh sandwiches, we investigated the magnetic nature of the interfaces. Section 3.1 will be devoted to the magnetic moment profile. The variation of the saturation magnetisation with the Co thickness for a series of Co single layers indicates that there is no reduction in the Co moment even at the Co/Rh interfaces. This is supported by *ab initio* calculations of the magnetisation with mixed interfaces which show that even for a mixed monolayer of 75% of Rh and only 25% of Co, the Co moment remains close to the bulk value. Section 3.2 presents the magnetoresistance results which confirm the good quality of the magnetic interfaces.

2 Preparation conditions and structural characterisations

2.1 MBE grown Co/Rh sandwiches

A serie of samples with the following composition: [100 Å Rh 32 Å Co x Å Rh 32 Å Co 24 Å Rh] was prepared by e-beam evaporation on mica substrates in a ultra high vacuum (UHV) chamber with a background pressure of 4×10^{-10} torr. Six mica substrates of 1 inch diameter were freshly cleaved and immediately afterwards transferred to the chamber. They were then heated to 700 °C for 30 min to desorb surface contaminants. The RHEED pattern showed thin streaks and Kikuchi lines which indicate large flat surface areas. Mica substrates exhibit a pseudo hexagonal surface structure which causes the densely packed (111) and (0001) atomic planes of deposited fcc and hcp metals respectively to align parallel to the substrate surface.

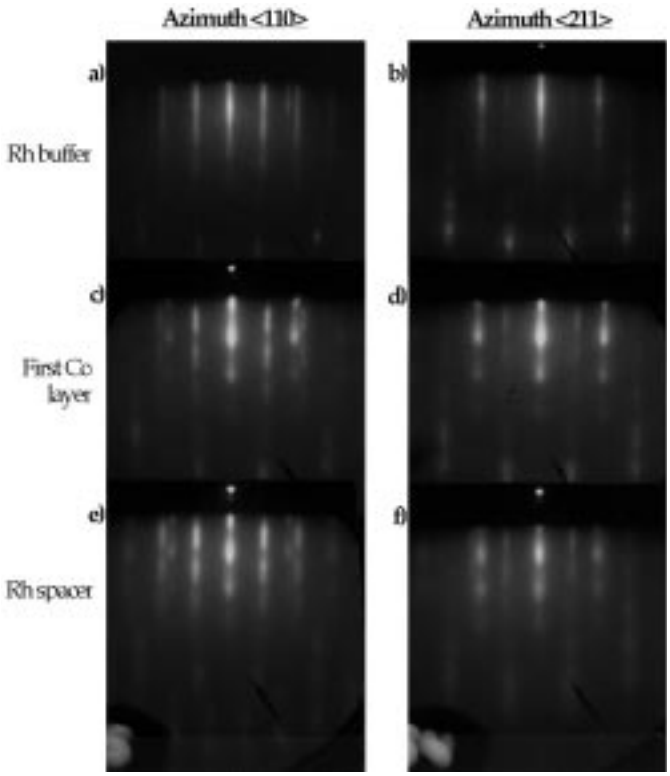

Fig. 1. RHEED images for completed layers of an MBE grown Co/Rh sandwich with a Rh (111) buffer layer deposited on a mica substrate along two principal azimuths.

A 100 Å thick Rh (111) buffer layer was deposited onto six mica substrates simultaneously at a temperature of 700 °C at a rate of 2 Å/min and a vacuum pressure of about 6×10^{-10} torr. The thickness was monitored using a quartz crystal oscillator and the samples were rotated during the growth. The RHEED pattern of the mica substrates vanished quickly and diffraction streaks re-emerged only after deposition of about 50 Å of Rh. As the Rh film thickness increases, the width of the streaks decreases continuously indicating that atomically ordered regions become larger.

The RHEED patterns for the completed Rh (111) buffer layer along the $\langle 110 \rangle$ and $\langle 211 \rangle$ azimuths (Figs. 1a and 1b) are well defined and characteristic of an ordered single crystal. The separation of the streaks along the $\langle 110 \rangle$ azimuth is proportional to $1/a_{\langle 110 \rangle}$ whereby $a_{\langle 110 \rangle} = a_{\mathrm{Rh}}/\sqrt{2} = 2.69$ Å is the nearest neighbour distance in the densely packed fcc(111) plane. The corresponding streak separation along the $\langle 211 \rangle$ azimuth is $1/a_{\langle 211 \rangle} = 1/\left(\sqrt{3} \times a_{\langle 211 \rangle}\right)$. In Figure 1a, two additional faint streaks are visible in the zeroth order Laue zone. Their distance from the specular streak is $\sqrt{3}$ times as

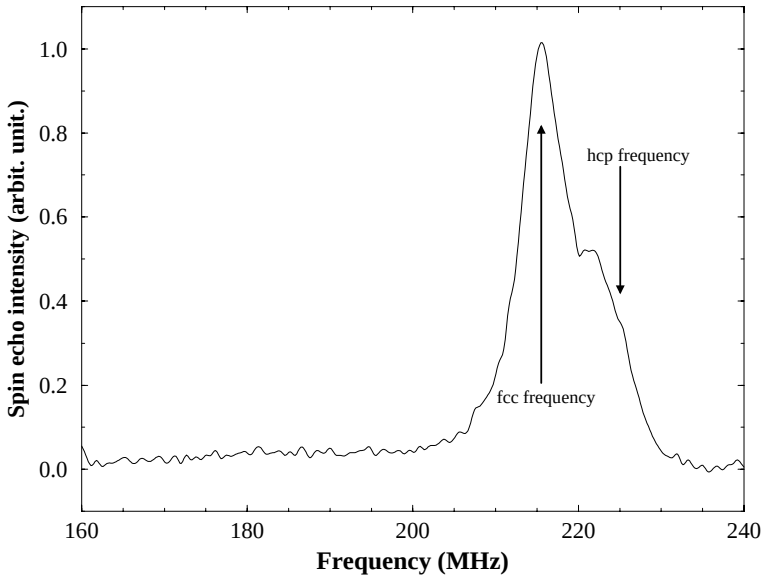

Fig. 2. Co NMR spectrum of the MBE grown Co(32 Å)/Rh(19 Å)/ Co(32 Å) sandwich.

large as the separation between the intense streaks. Thus, the faint streaks represent diffraction from a surface area with the ⟨211⟩ crystal direction perpendicular to the incident electron beam. This indicates the presence of small structural domains which are rotated through 30° with respect to the dominating surface orientation.

The first 32 Å thick Co layer was deposited at room temperature at a rate of 5 Å/min, with a vacuum pressure of about 4×10^{-10} torr. Detailed RHEED analysis of this layer performed during the growth have indicated that the relaxation of the Co layer occurs after about five or six monolayers. This result is similar to what has been observed on the Co/Ru system [8]. RHEED patterns for this Co layer are shown for both crystal directions in Figures 1c and 1d. The streak spacing has increased by 8.5% with respect to the Rh buffer layer, which gives rise to a nearest neighbour distance in the hexagonal Co plane of 2.48 Å, close to the value expected for bulk Co (2.51 Å). Compared with the Rh buffer, the streaks have become broader and spottier. While the latter suggests that the Co surface is rougher, the former indicates that crystalline regions of Co are smaller than for the Rh buffer. Thus Co on Rh does not grow in the ideal layer-by-layer mode and island formation occurs. In fact, the surface energies of Co and Rh are very similar in contrast to the Co/Cu or Co/Ru systems for which narrower streaks for the Co layers are observed [8,9]. The stacking sequence along the (111) growth direction can be determined from the intensity modulation along the RHEED streaks. The elongated double spots on the first RHEED streaks next to the specular streak in Figure 1c clearly indicate that Co has grown in the fcc phase.

As for the Rh buffer layer, in Figure 1c additional spotty streaks are observed on the RHEED patterns along the ⟨110⟩ azimuth and corresponds to the contribution of the ⟨211⟩ azimuth. *Vice versa*, intermediate streaks are visible in Figure 1d along the ⟨211⟩ RHEED pattern, which can be assigned to the ⟨110⟩ azimuth. Thus, growth continues for the two orientational domains which are rotated by 30° with respect to each other and which were observed already for the Rh buffer. However, those additional structures appear only for very small angles between the incident 30 keV electron beam and the surface plane, which indicates that they do not extend throughout the whole film thickness and they subsist as surface effects.

The Rh spacer layers with thicknesses ranging from 4 Å to 29 Å are deposited at room temperature at a rate of 2 Å/min and a vacuum pressure of about 4×10^{-10} torr. The RHEED streaks have hardly changed (Figs. 1e and 1f) with respect to the first Co-layer. Thus, the Co surface is not smoothed by a Rh overlayer, the crystal structure remains fcc, and the two orientational domains persist.

The second 32 Å thick Co-layer and the 24 Å thick Rh protection layer have been deposited under the conditions given above for the corresponding material. The RHEED patterns do not degrade further, and continue to show fcc islands and two orientational domains.

Zero field NMR measurements have been performed at 1.5 K with a broad band pulsed NMR spectrometer in order to confirm the fcc structure of the Co layers. The NMR spectra of the MBE-grown $Co_{32\ Å}/Rh_{19\ Å}/Co_{32\ Å}$ sandwich in Figure 2 shows a clear main resonance line at a frequency of 217 MHz. This frequency is close to the bulk fcc Co NMR frequency (216 MHz) which indicates that the Co layers are stabilised in the fcc structure, in agreement with RHEED observations. The presence of a shoulder at the right side of the main line is characteristic of stacking faults which give rise in general to NMR lines lying between the fcc and hcp (228 MHz) Co lines. It can also be noted that there is no tail below the main line which would be due to the contribution of Co atoms at the interfaces with Rh atoms as nearest neighbours.

We have then prepared CoRh alloys with small Rh concentration to study the evolution of the Co resonance frequency as a function of the number of Rh nearest neighbours. The obtained NMR spectra show that the resonance frequency of the Co atoms with one, two or three Rh atoms as nearest neighbours is close to the bulk pure Co. This explains the fact that additional resonance lines have not been observed below the main line for the Co/Rh sandwich. This can be related, as we shall see in the next section, to the fact that Co atoms preserve their moments at the interfaces even in the case of large interfacial diffusion. As a consequence, the NMR spectra do not allow a quantitative determination of the topology of the interfaces. The similarity between the phase diagrams for the CoRu and CoRh alloy may indicate the presence of intermixing at the Co/Rh interfaces since a large intermixing at the Co/Ru interfaces was found in the Co/Ru sandwiches [10].

2.2 Sputtered Co/Rh sandwiches

The layers were deposited by DC magnetron sputtering for Co and RF sputtering for Rh on silicon oxide substrates, which provides homogeneous stacks with a thickness fluctuation below 1%. The base pressure was 4×10^{-7} torr and the Ar pressure was 10^{-2} torr. The sample holder was rotating during the sputtering process. A series of sandwiches with the same geometry as for the MBE grown sandwiches was prepared in order to study the effect of the growth conditions on the interlayer coupling strength. For X-ray diffraction analysis, a multilayer with the geometry 100 Å Rh / [30 Å Co / 9 Å Rh]$_{15}$ / 20 Å Rh was grown. To study the magnetic quality of the interfaces, an additional series of Co single layers was deposited on a 100 Å Rh buffer layer and covered by a 30 Å Rh protection layer with Co thicknesses varying from 10 to 70 Å.

X-ray measurements were carried out using a high resolution X-ray Philips diffractometer. The geometry of the diffractometer allows only experiments in the reflection mode. We performed both high-angle and small-angle $q/2q$ scans around the first-order Bragg peak. The small-angle spectrum in Figure 3a shows the presence of Kiessig fringes indicating a limited surface roughness. The high-angle spectrum in Figure 3b shows a well defined main Bragg peak for $2q = 43.6°$ and indicates a preferential (111) texture in the Co/Rh layers. The figure shows also the presence of satellites at each side of the main peak which is direct evidence of the composition modulation. The best fit of the experimental data shown in Figure 3 leads to the main Bragg peak with a parameter corresponding to the fcc [111] growth direction. This result indicates that the Co/Rh MBE-grown and sputtered sandwiches have a similar texture.

3 Magnetic and transport properties

The resistance of the samples was measured using a four-probe low-frequency ac lock-in technique with spring-loaded gold-plated contacts. For the samples which show saturation fields larger than 2 T, the measurements were performed at the Service National des Champs Magnétiques Pulsés (SNCMP) in Toulouse (France) in the slow decreasing part of a pulsed field cycle (field rise time: 5 ms, field decay time: 500 ms) with the maximum field reaching 35 T. All magnetoresistance data were measured at 300 K with the magnetic field applied in the film plane and parallel to the current direction. Magnetisation measurements were performed using alternating gradient force (AGFM) and SQUID magnetometry. The saturation field is defined as the field at which the resistance curve first deviates from the high field slope. This ensures that this critical field is close to the exchange field. Indeed, small angles between the magnetisation of successive magnetic layers have more impact on the resistivity of the sample than on its total magnetisation. Thus, the saturation field is more accurately defined from GMR curves than from the magnetisation curves.

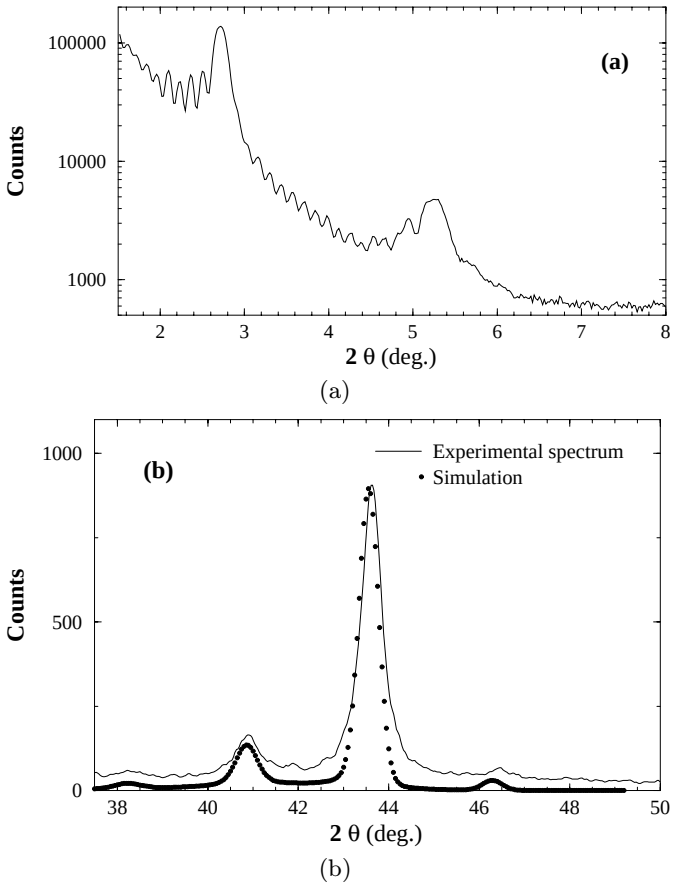

Fig. 3. X-ray diffraction spectrum recorded for 100 Å Rh / [30 Å Co / 9 Å Rh]$_{15}$/ 20 Å Rh multilayer. (a) small-angle spectrum, (b) high angle spectrum.

Figure 4a shows the variation of the saturation field (H_s), measured at 300 K, for the series of MBE grown and sputtered Co/Rh sandwiches as a function of the Rh spacer layer thickness. The following differences between the MBE grown and the sputtered samples can be observed: (i) The first antiferromagnetic peak occurs at 8 Å Rh for the sputtered samples, while the exchange

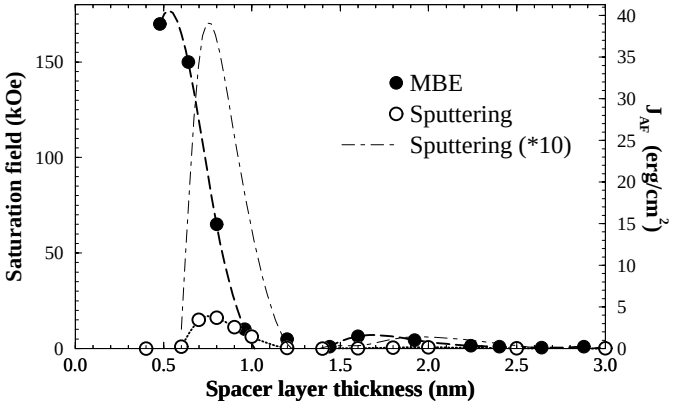

(a)

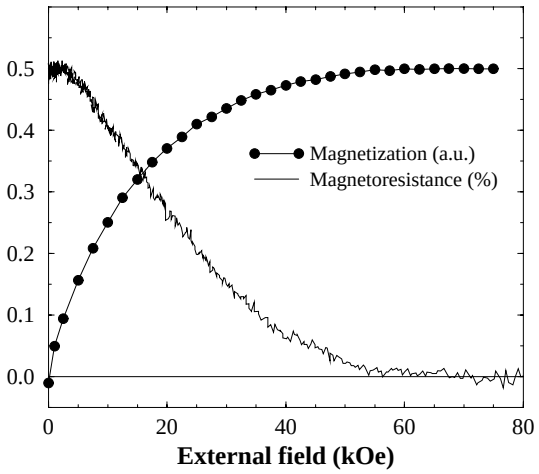

(b)

Fig. 4. (a) Variation of the saturation field (H_s) and antiferromagnetic exchange coupling J_{AF} of two series of twelve MBE grown and sputtered Co/Rh sandwiches as a function of Rh spacer layer thickness at 300 K. (b) Magnetisation and magnetoresistance curves for the MBE grown Co(32 Å)/Rh(8 Å)/ Co(32 Å) sandwich. The zero MR line is plotted to show that the saturation is determined as the value at which the MR curve deviates from this line.

coupling field increases continuously with decreasing Rh thickness for the evaporated samples down to the 5 Å Rh thick sample, which corresponds to the thinnest investigated sample. Thus the thickness for the appearence of the antiferromagnetic coupling is different between the two series, which is the first consequence of the structural quality on the interlayer coupling; (*ii*) The most striking result in Figure 4a is the very large saturation field close to 170 kOe observed for the sample with a Rh spacer layer thickness of about 5 Å. Due to the high field SQUID limitation (80 kOe maximum field), the saturation of the magnetisation curves have only been deduced for samples with Rh spacer layers thicker than 7 Å. For thinner Rh layers, the saturation fields have been determined from the magnetoresistance (MR) curves using the pulsed field facilities in Toulouse.

The saturation field reflects the maximum strength of the antiferromagnetic interlayer exchange coupling (J_{AF}) as $J_{AF} = H_s M_s t_{\mathrm{Co}}/2$, where M_s and t_{Co} are the saturation magnetisation and thickness of the magnetic layer respectively. Indeed, the shape of both magnetisation and magnetoresistance curves (Fig. 4b) suggests that the coupling is not homogeneous across the samples. We have used a model allowing bilinear, biquadratic and anisotropic terms [10]. This model has shown, by successfully fitting the rounded magnetization curves in the case of the Co/Ru system, that a biquadratic coupling term exists in a very narrow range of thicknesses between 4 and 6 Å. However, this model was unsuccessful in fitting the rounded magnetization and magnetoresistance curves in the case of the Co/Rh system which implies that a more complicated mechanism takes place, certainly due to the distribution of coupling strengths. A possible explanation of this mechanism is related to the different nature of the magnetic interfaces for Co/Ru and Co/Rh. In both cases, the profile of the interfaces is consistent with a fluctuation of the concentration over a few atomic %. In this case, J_{AF} represents the maximum coupling value that can be reached in the sample. With these considerations and on the basis of the experimental data, the exchange constant value (J_{AF}) found for the evaporated sandwich ($t_{\mathrm{Rh}} = 4.8$ Å) is equal to 39 erg/cm^2 at 300 K. To our knowledge, such a giant indirect exchange coupling is observed for the first time in this kind of artificial structure, and is much stronger than the largest antiferromagnetic exchange coupling values found in MBE grown Co/Ru sandwiches (4.5 erg/cm^2) [11] or in sputtered Co/Ru multilayers (5 erg/cm^2) [2]. For the sputtered series, the antiferromagnetic coupling reaches its maximum value (3.4 erg/cm^2) for a Rh thickness of about 8 Å. Again this coupling is stronger than the value (1.6 erg/cm^2) reported previously [6] for Co/Rh sputtered multilayers with the same Rh thickness but approximately ten times smaller than the value observed for the MBE grown sandwiches. This result is evidence of the effect of the structural quality, and particularly the interface morphology, on the interlayer coupling strength. Figure 4 shows that the strongest antiferromagnetic coupling is observed for the thinnest Rh layer investigated ($t_{\mathrm{Rh}} = 4.8$ Å) for MBE grown sandwiches as opposed to the sputtered sandwiches for which the coupling is ferromagnetic for 4 Å and 6 Å of Rh thicknesses. This is also an indication of the influence of the interdiffusion and the morphology of the interfaces on the antiferromagnetic coupling which shifts the appearance of the coupling to higher thicknesses.

This can be further confirmed after a close look on the magnetisation curves measured at room temperature with the magnetic field applied in the film plane (Figs. 5 and 6). For sputtered samples, the magnetisation curves in Figure 5 show a high remanence even for the strongly antiferromagnetically coupled sandwich with 8 Å Rh ($Mr/Ms = 0.2$). As reported in Figure 7, this remanence decreases as the Rh thickness increases and vanishes for Rh thicknesses larger than 10 Å. In contrast, for the evaporated sandwiches (Figs. 6 and 7) the remanence is smaller and disappears for thinner Rh thicknesses.

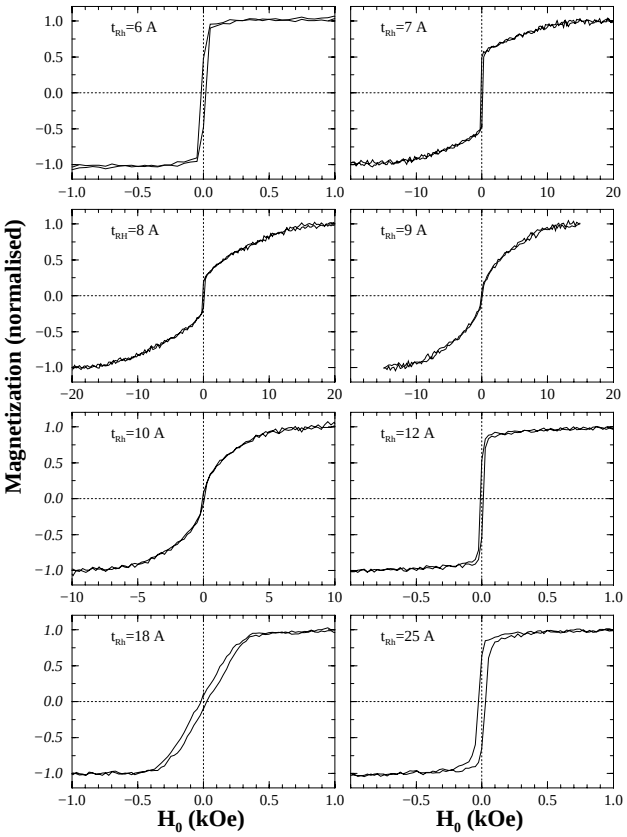

Fig. 5. Magnetisation curves measured at 300 K with the magnetic field applied in the film plane for several sputtered Co/Rh sandwiches.

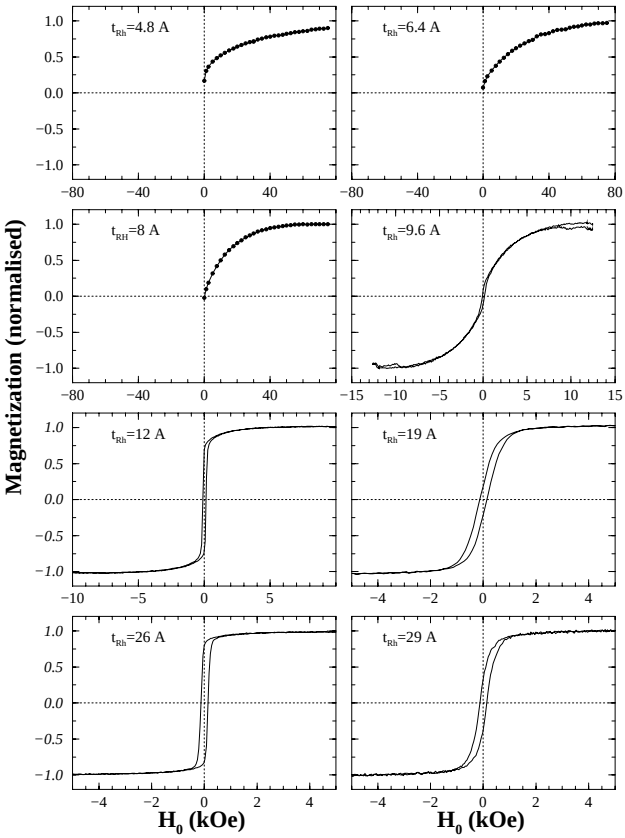

Fig. 6. Magnetisation curves measured at 300 K with the magnetic field applied in the film plane for several MBE grown Co/Rh sandwiches.

For $t_{\mathrm{Rh}} = 8$ Å, there is no more remanence. Such results are strong indications of the difference in the interface roughness between the evaporated and sputtered samples.

This assumption is supported by *ab initio* calculations of the coupling on Co_3Rh_n superlattices [12]. We use the first principle Augmented Spherical Wave technique and the Local Spin Density Approximation (LSDA) formalism for treating exchange and correlation of a many body electron system which allows the determination of the electronic structure of the superlattices. It has been shown that this method is well suited to study the magnetic interlayer exchange coupling in various superlattice systems such as Fe/Pd [13,14], Fe/Cr [15], Fe/Mn [16], Co/Cu [17, 18] and Co/Ru [19].

A systematic study of the exchange coupling for varying Rh thicknesses was performed in the hcp stack of the Co/Rh superlattice. The calculation for the hcp structure requires only a double cell in the antiferromagnetic arrangement, the calculation for both the ferro and antiferromagnetic structure being performed for the following cell $2 \times [Co_3/Rh_n]$ with $n = 1, 2, 3, 4, 5, 6$. However, similar calculation in the fcc (111) structure needs a sextuple cell $6 \times [Co_3/Rh_n]$ with $n = 1, 2, 4, 5$ because of translational symmetry conditions. Such calculations require a large number of atoms in each unit cell, much larger than the maximum number of atoms allowed by the programme for reliable calculation ($N_{max} = 32$). As a consequence, only specific structures were calculated in the fcc stack, those which require just a double cell, $2 \times [Co_5/Rh_1]$, $2 \times [Co_4/Rh_2]$, $2 \times [Co_3/Rh_3]$.

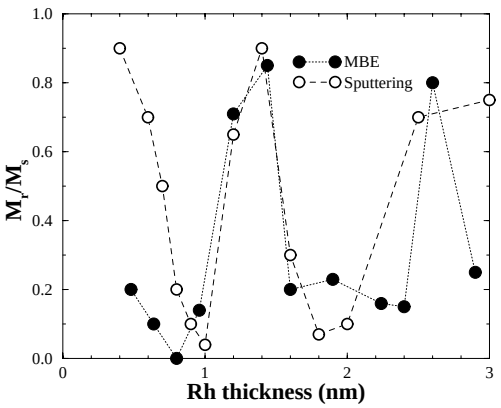

Fig. 7. Variation of the magnetic remanence as a function of Rh thickness for the sputtered (open circles) and MBE grown (full circles) sandwiches.

We determine the interlayer coupling by calculating the energy difference $\Delta E_{F-AF} = E_F - E_{AF}$ between the total energies obtained for the two opposite interlayer magnetic arrangements F and AF. The F (AF) interlayer magnetic arrangements correspond to parallel (antiparallel) magnetisation of successive cobalt

Table 1. Experimental J_{exp} (erg/cm^2) and theoretical J_{th} (erg/cm^2) magnitude of the antiferromagnetic exchange coupling and GMR signal for Co/Ru and Co/Rh systems in both fcc and hcp configurations.

	J_{th} (erg/cm^2)	J_{exp} (erg/cm^2)	GMR (%)	Thickness (Å)	reference
Co/Ru (hcp)	-	5 (4.2 K)	6.5	3	[2] (multilayers)
	-	0.5 (300 K)	-	4	[4]
	-	4.5 (300 K)	0.1	5	[11]
	95	-	-	2	This work
Co/Rh (hcp)	38	-	-	4	This work
Co/Rh (fcc)	27	-	-	4	This work
	-	39	0.5	5	This work
	-	1.6	-	7.9	[7]

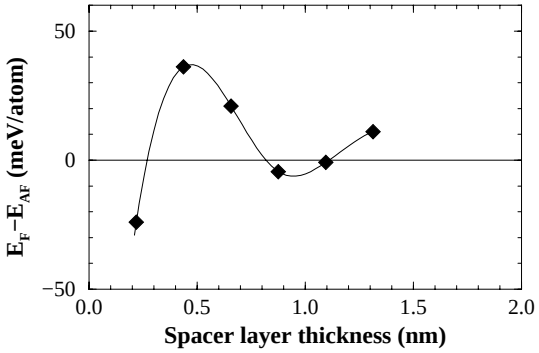

Fig. 8. Variation in the energy difference between the ferromagnetic and antiferromagnetic state as a function of the spacer layer thickness for a perfect Co_3Rh_n superlattices.

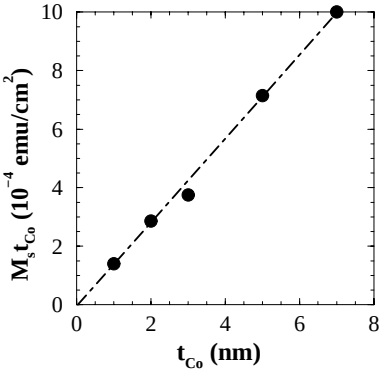

Fig. 9. Variation in the measured saturation magnetisation per unit surface of Co, $M_S t_{\mathrm{Co}}$, with Co layer thickness t_{Co} for mica/Rh (150 Å)/ Co (t Å)/Rh (50 Å) Co single layers at $T = 300$ K.

layers. The interlayer coupling J deduced from $\Delta E = J \times M1 \times M2/(M1 \times M2)$ is calculated from the energy difference $\Delta E_{F-AF} = 2J$ (according to the definition of J in Ref. [20], the energy difference per unit cell is $2J$ for one Rh layer and $4J$ for the total antiferromagnetic cell). Figure 8 shows the variation of the exchange coupling J as a function of the Rh spacer layer thickness in the hcp stacking while Table 1 gives the values of the exchange coupling for some specific fcc stacking structures. To compare quantitatively the values obtained theoretically with the experimental data, we have expressed the meV/(crystallographic cell) unit in erg/cm^2 [21]. The calculated coupling shows an oscillatory behaviour with a period of about 5 Rh monolayers and a first antiferromagnetic maximum for 2 atomic layers of Rh (corresponding to a 4 Å Rh thick layer). The value obtained for the hcp stacking for the Co_3Rh_2 equal to 38 erg/cm^2 can be compared directly to the value obtained for the fcc stacking for the Co_4Rh_2 (27 erg/cm^2). This slight difference between both values is due to (*i*) the structures, the stacking differs from the ABAB... to the ABCAB... one while the atomic planes are strictly the same, and also (*ii*) to the variation of the magnetic layer thickness from 3 to 5 cobalt atomic planes [22–24]. The comparison between the experimental and theoretical values shows a very satisfactory agreement. To our knowledge, first principles calculations have always shown the coupling to be several orders of magnitude higher than measured in different multilayered systems, Fe/Cr [15,25–27], Co/Cu [28,22,29], Co/Ru [19,30, 31]. This striking agreement is certainly due to the fact that for the first time a very strong coupling has been found experimentally and can be attributed to the nature of the magnetic/non-magnetic interfaces. This will be discussed in the next part of the paper. Furthermore, the theoretically predicted phase of the coupling agrees well with the experimental one, particularly for the MBE-grown samples. We have observed, experimentally, an antiferromagnetic coupling for the thin Rh spacer layers (between 4.8 and 9.6 Å), then a large remanence for the sample with 12 Å Rh, indicating that this sample is mostly ferromagnetically coupled and again an antiferromagnetic coupling for thicker spacers. Thus, there is an experimental oscillatory exchange coupling with a period of about 10 Å. The only difference with the theoretical behaviour is the antiferromagnetic coupling for 9.6 Å Rh, while a ferromagnetic coupling is predicted for this thickness, indicating that there is a slight shift of the phase (or period) between the theory and the experiment.

3.1 Interfacial magnetic properties

Figure 9 shows the variation of the saturation magnetic moment surface density of Co, $M_s t_{\mathrm{Co}}$, *versus* cobalt thickness (t_{Co}) for mica/Rh (150 Å) /Co (t_{Co} Å) /Rh (50 Å)

single magnetic layers. The linear decrease in the magnetisation with decreasing t_{Co} is expressed by a linear function which intercepts the abscissa at a thickness of 0 Å Co. This indicates that there is no reduction in the magnetisation for Co atoms located at the Co/Rh interfaces despite the fact that the CoRh phase diagram is similar to that for CoRu and hence mixing at the interfaces is expected. This result suggests that intermixing is not incompatible with the preserved Co moment even when Co atoms are mixed with a large concentration of Rh at the interfaces. To confirm this result, the magnetic moment profile was determined from the previous calculations. The profile was calculated for mixed interfaces and the moments determined self- consistently on each atomic site. The cell contains 32 inequivalent atoms (4 atoms per in-plane cell) as shown in Figure 10 and the band structure was computed with approximately 300 k-points in the irreducible part of the Brillouin zone. We estimate the accuracy on the magnetic moment values to be better than 0.01 μ_B [32]. To give a comparison with the experimental results, we have used mixed interfaces on the basis of the linear profile determined by NMR measurements on Co/Ru sandwiches [10] for the following structure (see Fig. 10):

$$Co/Co/Co/Co_{0.75}Rh_{0.25}/Co_{0.5}R_{0.5}/Co_{0.25}Rh_{0.75}/Rh/Rh.$$

The same profile as the one determined experimentally for the Co/Ru system [33] has been chosen because of the possibility to make a direct comparison between both systems (Co/Ru and Co/Rh) and of the simplicity of the cell (a fcc Co/Rh stacking gives very similar results [34]).

The results of the calculations are shown in Figure 11, which presents the evolution of the local magnetic moment for all atoms in the stack as a function of their position. The horizontal dashed line corresponds to the bulk Co moment value. As can be seen in Figure 11, the Co moment value remains approximately the same (close to the bulk value) even for the atomic layers with a large Rh concentration (75 at% Rh) (between vertical lines 5 and 6 in Fig. 11). This result differs from the profile calculated for the Co/Ru system, shown in Figure 11, for which the Co moment decreases continuously as a function of the Ru concentration and vanishes almost completely for high Ru concentration (75 at% Ru) [12]. These results are in good agreement with the experimental data discussed above and confirm the compatibility between mixed interfaces and preservation of the local magnetic moments. In addition, the Rh polarization is large (and positive): 0.65 μ_B for 25 at% Rh (between vertical lines 3 and 4 in Fig. 11) and 0.25 μ_B for 75 at% Rh (between vertical lines 5 and 6 in Fig. 11). This is in good agrement with recent experiments reported by Gallet *et al.* [35] in CoRh alloys which have shown that Rh is strongly polarized with a magnetic moment of 0.6 μ_B. Blügel [36] has also shown the high degree of polarization of Rh monolayers on Ag (001). Such a high polarization of Rh atoms in our case finds its origin in the proximity of the Co atoms with a conserved moment. Indeed, for pure Rh (or Ru) planes (between vertical lines 6 and 7 in Fig. 11) there is no difference between Rh and Ru moments, while for the next pure Rh (or Ru) plane (between vertical lines 7 and 8 in Fig. 11) close to the pure Co plane, the moment on the Rh atoms present a large value 0.25 μ_B compared to 0 μ_B on the Ru atoms. These results enforce our hypothesis that the magnetic nature of the magnetic/non-magnetic Co/Rh interfaces is probably at the origin of the unexpected giant interlayer exchange coupling strength observed for this system.

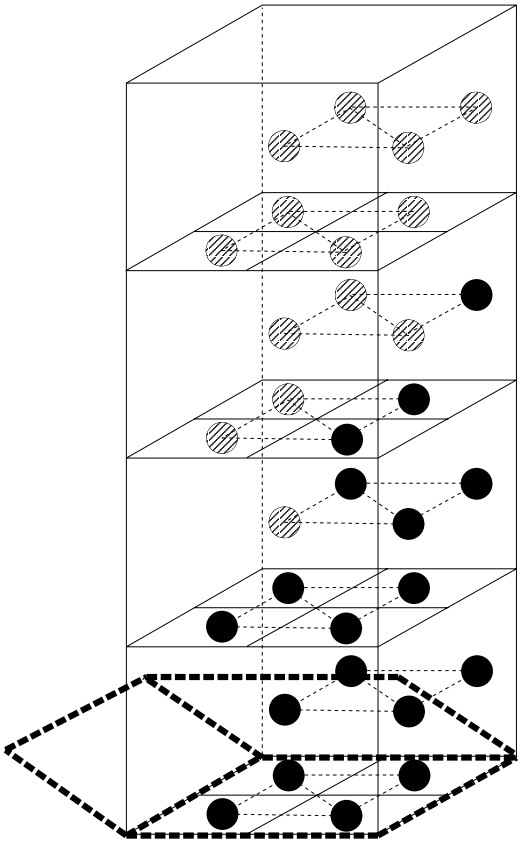

Fig. 10. Schematic view of the cell used for the magnetic profile calculation which contains 32 inequivalent atoms. 4 atoms per in-plane cell. Co atoms (full circles) and Rh (Ru) (dashed circles).

The results presented in the last sections have shown that a giant antiferromagnetic coupling strength and preserved local magnetic moments near the magnetic/non-magnetic interfaces are observed simultaneously in the evaporated Co(32 Å) /Rh(t_{Rh})/Co(32 Å) sandwich. To understand the origin of these effects and to discuss their relation, we do a comprehensive comparison between the Co/Rh and Co/Ru systems.

The high antiferromagnetic coupling strength in sandwich and multilayer systems was first discovered in Co/Ru multilayers (5 erg/cm^2) [2] and sandwiches

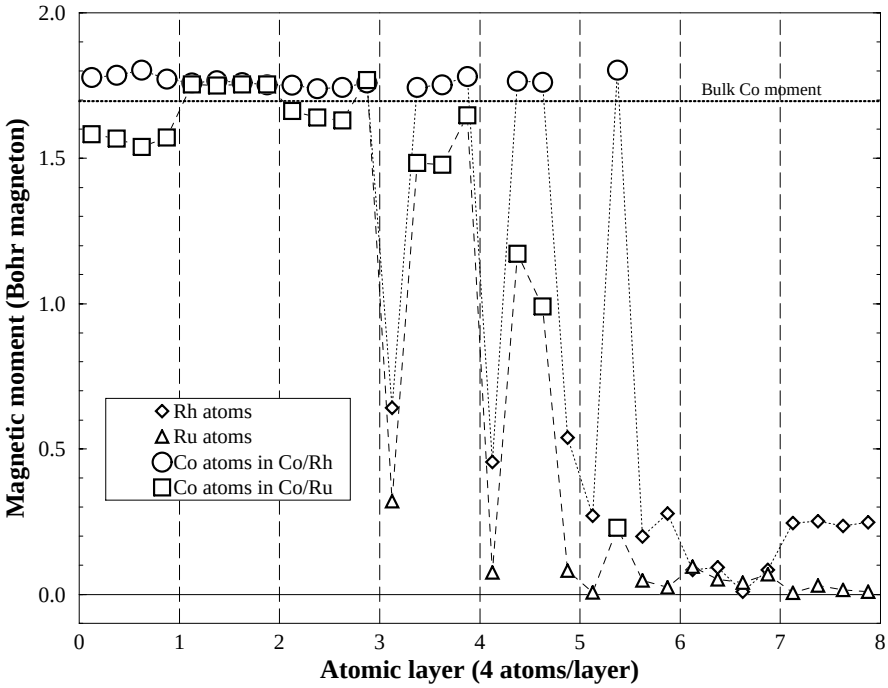

Fig. 11. Evolution of the magnetic moment as a function of the position of the Co atoms in the following stacks: $Co/Co/Co/Co_{0.75}M_{0.25}/Co_{0.5}M_{0.5}/Co_{0.25}M_{0.75}/M/M$, with M = Ru or Rh, from *ab initio* calculations. The horizontal dashed line corresponds to the bulk Co moment value.

(4.5 erg/cm^2) [11]. These values are approximately 8 times smaller than the value observed in Co/Rh sandwiches. This large difference between both systems finds its origin in the magnetic nature of the interfaces. Indeed, the experimental study of the Co/Ru sandwiches has shown that the Co/Ru interfaces are intermixed along three monolayers. The calculation of the magnetisation with mixed interfaces has shown that the Co moment for the Co atoms located at the interfaces decreases continuously with increasing the Ru concentration in the considered layer and disappears completely for high Ru concentrations (Fig. 11). This was in agreement with magnetisation measurements which have shown that 2 Å of Co are magnetically dead at each interface.

To understand the differences in the coupling observed between the Co/Ru and the Co/Rh from an electronic structure viewpoint, we have determined the density of states (LDOS) for Co/Rh and Co/Ru sandwiches reported in Figures 12 and 13 for mixed interfaces as described in Figure 10. The comparison of Figures 12 and 13 shows that several factors are at the origin of the differences in the electronic structure of the considered interfaces. The polarisation capability of the spacer element, the hybridisation between Co and spacer material, the preservation of the local magnetic moments, and the band matching of the densities of states have all to be considered.

It is well-known that Rh has a higher magnetic susceptibility than Ru. This is reflected in Figure 11 by a much larger induced magnetic moment on the Rh site (0.65 μ_B) than on the Ru site (0.3 μ_B) in the first mixed layer (I) with $Co_{75\%}$ (Ru or Rh)$_{25\%}$ (between vertical lines 3 and 4 in Fig. 11). As a consequence, the magnetic Rh atoms have a LDOS which presents a significant asymmetry in the spin up and down bands and matches the Co densities of states better than for the case of Ru. Moreover, the bulk bandwidth for Rh is smaller than for Ru, resulting in a smaller enhancement of the bandwidth of the LDOS on the intermixed Co sites. Consequently, the Co-Rh hybridisation is qualitatively less destructive, from the view point of the Stoner criterion, for the magnetism of the Co atoms in the mixed zone than the Co-Ru hybridisation. Most of the LDOS characteristics can be explained by these qualitative arguments. It is interesting to note that the minority bands are the most different between Ru and Rh, the majority bands being very similar. When the first mixed plane (Plane I, between vertical lines 3 and 4 in Fig. 11) shows only slight differences, the LDOS on the second plane (Plane II, between vertical lines 4 and 5 in Fig. 11) with $Co_{50\%}$ (Ru or Rh)$_{50\%}$ exhibits significant modifications in the electronic structure. The LDOS on the Co sites in the mixed zone are less asymmetric for both spin direction for Ru than for Rh: this is a direct consequence of the destructive character of the Co/Ru hybridisation for the Co magnetism. The differences in the LDOS are found to be larger for the third mixed plane (Plane III, between vertical lines 5 and 6 in Fig. 11) $Co_{25\%}$ (Ru or Rh)$_{75\%}$. Effectively, the Co atom is nearly non magnetic when mixed with Ru and the spin up and down LDOS are very similar whereas for the Co atom mixed with Rh, the LDOS remains nearly unchanged as compared to the other mixed planes. This is a consequence of the preserved Co magnetism.

The coupling strength can also be qualitatively understood in terms of preserved magnetism and higher spin

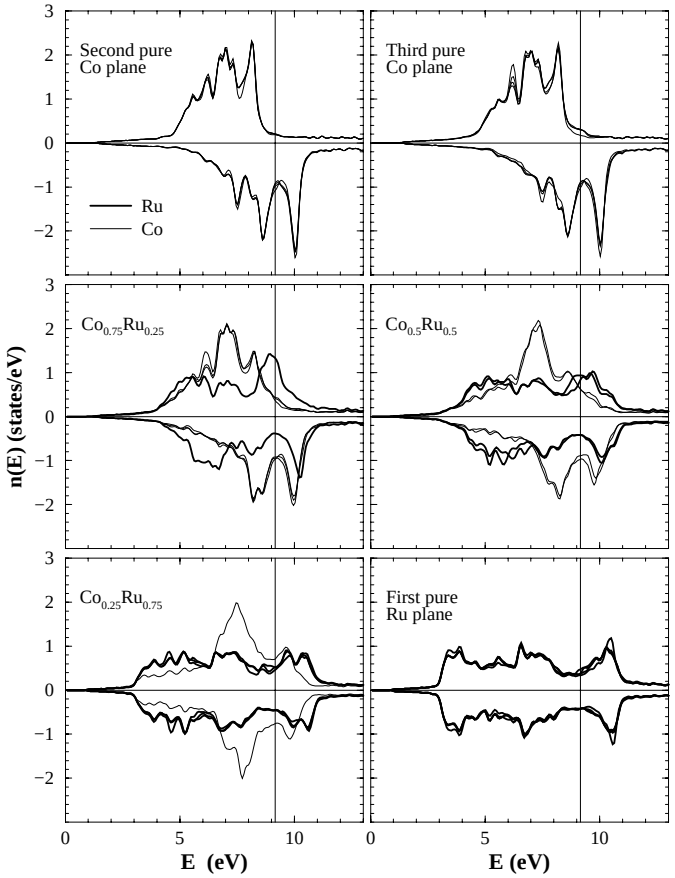

Fig. 12. Density of states calculation for Co/Ru sandwiches using the following stacks: Co/Co/Co/$Co_{0.75}$ $Ru_{0.25}$/$Co_{0.5}Ru_{0.5}$/$Co_{0.25}Ru_{0.75}$/Ru/Ru.

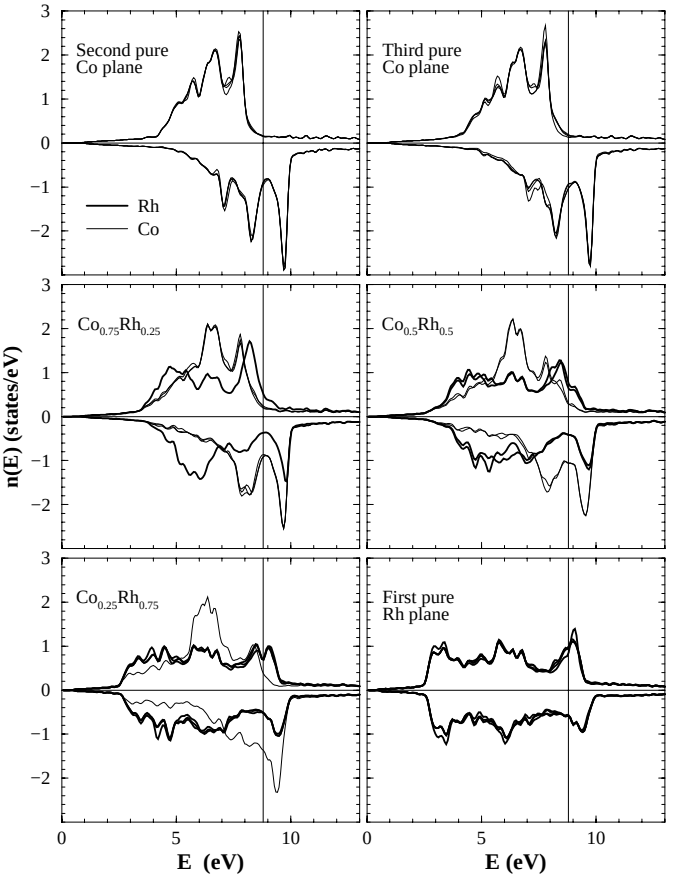

Fig. 13. Density of states calculation for Co/Rh sandwiches using the following stacks: Co/Co/Co/$Co_{0.75}$ $Rh_{0.25}$/$Co_{0.5}Rh_{0.5}$/$Co_{0.25}$ $Rh_{0.75}$/Rh/Rh.

assymmetry of the reflections at the Co/Rh interface. All theories agree to describe the interlayer exchange coupling for large spacer thicknesses in terms of spin asymmetric electronic confinement in the spacer layer [3,37]. The strength of the coupling is determined by the spin asymmetry $\Delta r = [r^{\uparrow} - r^{\downarrow}]/2$ of the electron wave function reflection amplitudes at each potential step [38] (the electrons of one spin type, the majority electrons of the Co are more strongly reflected). In the preasymptotic regime and in the case of a large polarisation of the spacer layer — which is the case under consideration in this paper — band matching between two bulk like wave functions cannot be assumed because of the absence of bulk like states within the spacer layer. However, the strength of the exchange coupling can be explained with the same ingredients *i.e.* in terms of quantum well states: the coupling strength is related to the spin asymmetry of the scattering potential steps $\Delta V = [\delta V^{\uparrow} - \delta V^{\downarrow}]/2$, δV^s being the potential step for the σ spin direction. Consequently, even if the coupling results from interference between different reflected contributions, it is reasonable to assume that the coupling gets stronger when $|\Delta V|$ is larger.

Each monolayer of the intermixed zone introduces supplementary potential steps (PS) which can be defined as PS1(X/Plane III), PS2(Plane III/Plane II), PS3(Plane II/Plane I) and PS4(Plane I/Co) with X= Ru or Rh. These potential steps add spin independent (*via* the average potential $\langle \delta V \rangle = (\delta V^{\uparrow} + \delta V^{\downarrow})/2$) and spin dependent (*via* ΔV) contributions to the confined wave function. Within a tight binding approach, the potential V can be evaluated for each intermixed plane by $V^{\uparrow}(V^{\downarrow}) = V(\mathrm{X}) + x \times V(\mathrm{Co}) - (+)(J/2)\langle M \rangle$, where x is the Co concentration, $\langle M \rangle$ the average local magnetic moment of the plane and J the effective exchange integral (which is on the order of 1 eV). As a consequence, the spin asymmetry of the potential step PSn is directly related to the average local magnetic moment variation by:

$$\Delta V = (J/2)(\langle M \rangle_{n+1} - \langle M \rangle_n).$$

The calculations betray a much stronger polarization of the Rh, and no loss in the cobalt magnetic moment thus indicating the stronger impact of an asymmetry on the electron confinement in the Co/Rh spacer. In contrast, for the Co/Ru system, reflections at PS1 have no spin asymmetry, are poorly spin asymmetric at PS2 and highly spin asymmetric at PS3 and PS4, whereas for the Co/Rh system, reflections at all potential steps are highly spin asymmetric. Finally, since the reflections at PS2, PS3 and PS4 occur on the transmitted fraction of the wave function, there is a significant reduction of the contributions

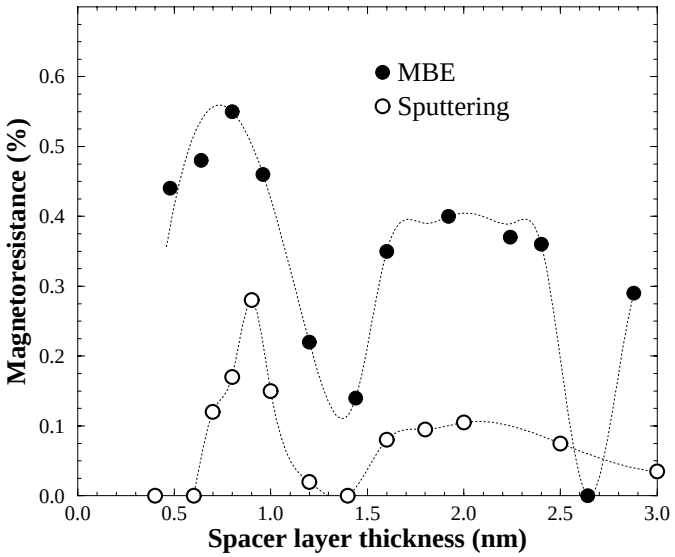

Fig. 14. Variation in the Magnetoresistance as a function of the Rh spacer layer for two series of twelve MBE grown and Sputtered sandwiches.

to the exchange coupling coming from PS$n+1$ as compared to PSn. Consequently, the coupling strength is enhanced when highly spin asymmetric reflections occur at the potential step PSn with the lowest index n as obtained for Co/Rh. This is not the case for Co/Ru where PS1 adds mainly a spin independent contribution to the confinement and affects only slightly the coupling strength.

All these theoretical considerations give strong support to the observation of a much stronger coupling strength in Co/Rh than in Co/Ru, the differences being due to a larger spin asymmetry in the scattering potential steps at the strongest contributing planes of the intermixed interfaces.

3.2 Magnetoresistance

Another signature of this effect is evidenced on the giant magnetoresistance results presented in Figure 14. This shows that the oscillations are similar to those for the coupling strength, deduced from the magnetisation curves. The second maximum shows a very peculiar behaviour with a large plateau of the MR values for Rh thicknesses above 15 Å, which is strikingly different from well defined peaks observed in other systems [Fe/Cr, Co/Cu, Co/Ru]. However, this second maximum is better defined for the MR than for interlayer coupling oscillations (Fig. 4). This can be explained by the fact that, first the MR is sensitive to relative orientations of the consecutive magnetic layers more than to the strength of the exchange coupling: the samples corresponding to the second peak present a well defined 100% antiferromagnetic coupling (strong enough to overcome the friction of the Co layers), which leads to MR values close to the ones of the first peak. Second, the good quality of the magnetic interfaces gives rise to an homogeneous magnetic orientation in the Co layers, even if the coupling is weaker, so the same MR value is reached for sandwiches around the second peak, since these samples have the same percentage of antiparallel aligned regions. This can also explain the decrease of the MR below 8 Å Rh for the evaporated samples while the exchange coupling continues to increase strongly. Indeed as shown in Figure 7, remanence starts to appear below 8 Å Rh, which indicates that the fraction of the sandwich with antiparallel magnetisation at zero field becomes smaller. The MR for MBE grown samples is approximately three times larger than for the sputtered samples which is evidence for the difference in the Co/Rh interface morphology between the two series and the difference of crystalline quality. On the other hand, the MR observed for the two Co/Rh series are very small and do not exceed 0.6%. Such a small GMR signal is not surprising since there is no asymmetry in the diffusion coefficients between the spin-up and spin-down: $\alpha = \rho^{\downarrow}/\rho^{\uparrow}$ is close to one for dilute Rh impurities in Co [39].

In summary, we present a giant indirect antiferromagnetic exchange coupling of 39 erg/cm^2 in fcc (111) epitaxial Co/Rh sandwiches which is ten times larger than the value observed for polycrystalline Co/Rh sandwiches. We explain this difference as being the consequence of the interfacial magnetism. By using magnetisation measurements and *ab initio* magnetisation calculations for the Co/Rh sandwiches we have evidence for a correlation between the magnetic nature of the magnetic/non-magnetic interface and the interlayer exchange coupling strength. We have shown that the sharper the magnetic nature of the interface is, the higher is the electronic confinement in the spacer layer and, consequently, the larger is the interlayer exchange coupling.

Parts of the *ab initio* calculations have been computed on the CRAY C98 of the Institut du Développement et des Ressources en Informatique Scientifique of the CNRS. This work was supported by the European Brite-Euram programme.

References

1. P. Grünberg, R. Schreiber, Y. Pang, M.B. Brodsky, H. Sower, Phys. Rev. Lett. **57**, 2442 (1986).
2. S.S.P. Parkin, N. More, K.P. Roche, Phys. Rev. Lett. **64**, 2304 (1990).
3. K. Ounadjela, D. Muller, A. Dinia, A. Arbaoui, P. Panissod, G. Suran, Phys. Rev. B **45**, 7768 (1992).
4. P.J.H. Bloemen, H.W. van Kerstern, H.J.M. Swagten, W.J.M. de Jonge, Phys. Rev. B **50**, 13505 (1994).
5. P. Bruno, C. Chappert, Phys. Rev. Lett. **67**, 1602 (1991).
6. J. Mathon, M. Villeret, D.M. Edwards, R.B. Muniz, J. Magn. Magn. Mater. **121**, 242 (1993).
7. S.S.P. Parkin, Phys. Rev. Lett. **67**, 3598 (1991).
8. D. Muller, K. Ounadjela, P. Vennegues, V. Pierron-Bohnes, A. Arbaoui, J.P. Jay, A. Dinia, P. Panissod, J. Magn. Magn. Mater. **104**, 1873 (1992).
9. N. Persat, A. Dinia, J.P. Jay, C. Mèny, P. Panissod, Thin

Solid Films, **275**, 115 (1996).
10. S. Zoll, H.A.M. van den Berg, J.P. Jay, H.J. Elmers, C. Mény, P. Panissod, D. Stoeffler, A. Dinia, K. Ounadjela, J. Magn. Magn. Mater. **156**, 231 (1996).
11. A. Dinia, K. Ounadjela, J. Magn. Magn. Mater, **146**, 66 (1995).
12. S. Zoll, *et al.* to be published.
13. D. Stoeffler, K. Ounadjela, J. Sticht, F. Gautier, Phys. Rev. B **49**, 299 (1994). D. Stoeffler, K. Ounadjela, J. Sticht, F. Gautier, J. Appl. Phys. **75**, 6467 (1994).
14. E. Fullerton, D. Stoeffler, K. Ounadjela, B. Heinrich, Z. Celinski, J.A.C. Bland, Phys. Rev. B **51** 6364 (1995).
15. F. Herman, J. Sticht, M.V. Schilfgraarde, J. Appl. Phys. **69**, 4786 (1991).
16. S.T. Purcell, M.T. Johnson, N.W.E. McGee, R. Coehoorn, W. Hoving, Phys. Rev. B **38**, 13064 (1992).
17. J. Kurdrnovsky, V. Drchal, P. Bruno, I. Turek, P. Weinberger, Phys. Rev. B **54**, 3738 (1996).
18. F. Herman, M.V. Schilfgraarde, J. Sticht, Int. J. Mod. Phys. B **7**, (1993).
19. D. Stoeffler, F. Gautier, J. Magn. Magn. Mater. **140**, 529 (1995).
20. K. Ounadjela, C.B. Sommers, A. Fert, D. Stoeffler, F. Gautier, V.L. Moruzzi, Europhys. Lett. **15**, 875 (1991).
21. 1 meV/atom = 2.52 erg/cm^2.
22. P.H. Bloemen, M.T. Johnson, M.T.H. van de Vorst, R. Coehoorn, J.J. de Vries, R. Jungblut, J. aan de Stegge, A. Reinders, W.J.M. de Jonge, Phys. Rev. Lett. **72**, 764 (1994).
23. P. Bruno, Europhys. Lett. **23**, 615 (1993).
24. L. Zhou, Z. Zhang, P.E. Wigen, K. Ounadjela, J. Appl. Phys. **76**, 7078 (1994).
25. M.V. Schilfgraarde, F. Herman, Phys. Rev. Lett. **71**, 1923 (1993).
26. S.T. Purcell, W. Folkertz, M.T. Johnson, N.E. McGee, K. Jager, J. aan de Stegge, W.B. Zeper, W. Hoving, P. Grünberg, Phys. Rev. B **46**, 261 (1992).
27. J. Unguris, R.J. Celotta, D.T. Pierce, Phys. Rev. Lett. **67**, 140 (1991).
28. F. Herman, J. Sticht, M. van Schifgaarde, J. Appl. Phys. **69**, 4783 (1991).
29. M.T. Johnson, R. Coehoorn, J.J. de Vries, N.W.E. McGee, J. ann de Stegge, P.J.H. Bloemen, Phys. Rev. Lett. **69**, 969 (1992).
30. Z. Zhang, L. Zhou, P. Wigen, K. Ounadjela, Phys. Rev. B **50**, 6094 (1994).
31. S. Zoll, H.A.M. van den Berg, K. Ounadjela, D. Stoeffler, A. Dinia, J. Appl. Phys. **79**, 2601 (1996).
32. D. Stoeffler, K. Ounadjela, J. Sticht, F. Gautier, Phys. Rev. B **49**, 299 (1994).
33. P. Panissod, *et al.* (private communication).
34. D. Stoeffler, *et al.* (to be published).
35. J.J. Gallet, J.M. Mariot, L. Journel, C.F. Hague, J.P. Kappler, G. Schmerber, D.J. Singh, G. Krill, J. Goulon, A. Rogalev, Phys. Rev. B **57**, 7835 (1998).
36. S. Blügel, Phys. Rev. B **51**, 2025 (1995).
37. P. Bruno, Phys. Rev. B, **411** (1995).
38. M. D. Stiles, Phys. Rev. B **48**, 7238 (1993).
39. I.A. Campbell, A. Fert, *Ferromagnetic Materiels* (North Holland, Amsterdam, 1982), p.769.